

TACTICAL TECHNICAL OFFICE Division

DARPA

Arlington, VA 22203-2114

DARPA-TR-17/006 September 30, 2017

DARPA-TTO

FINAL Report

MACE Proof-of-Concept – Superconducting Pulsed Transformer Study

by

Harry D. Fair, James Powell, John Mallick, and Jesse Powell



Approved for public release: distribution unlimited.

TABLE OF CONTENTS

1 Task Objectives	1
2 Technical Problems	2
3 General Methodology	2
4 Technical Results.....	3
4.1 Circuit Simulation and EM Modelling.....	3
4.2 Engineering Designs	11
5 Important Findings and Conclusions.....	15
5.1 Military Rationale	15
5.2 Design Requirements of MACE Demonstration Unit	17
5.3 Switching.....	21
5.4 Thermal Analysis	24
5.5 Structural Analysis	28
6 Significant Hardware Development	29
7 Special Comments	30
8 Implications for Further Research	30
8.1 MACE Prototype Development Roadmap.....	30
8.2 Phase 2: Key Suppliers, Subcontractors, and Facilities	31

1 TASK OBJECTIVES

The Institute for Strategic and Innovative Technologies (ISIT) proposed a new type of superconducting (SC) pulsed transformer which will demonstrate the highest energy density of any pulsed power technology. Phase I entitled “*MACE Proof of Concept – Demonstrate Fundamental Physics*” encompassed a six (6)-month effort to demonstrate the physics of a new type of high-energy-density SC pulsed transformer. The proposed SC pulsed transformer provided

a potential substantial reduction in size from the highest energy density state-of-the-art capacitor pulsed forming network (PFN) power source.

Phase I identified six (6) Milestones that marked completion of key stages of the project. These milestones are listed below:

1. Detailed project scoping
2. Characterization of MACE fundamental physics and analytical validation of MACE concept
3. Specification of MACE switching requirements
4. Specification of MACE cryogenic requirements
5. Characterization of expected MACE performance using CAD models and software simulation
6. Production of engineering designs and planning for Phase II

2 TECHNICAL PROBLEMS

The main technical problem addressed by the MACE feasibility study was to analyze, model, and simulate whether the MACE Superconducting Pulsed Power Transformer concept based on an annular (coaxial) primary/secondary coil assembly could repeatedly deliver a high percentage (>90%) of stored energy to an external load in under 10 milliseconds (ms).

3 GENERAL METHODOLOGY

In Phase I, ISIT conducted a non-experimental feasibility study of the MACE concept, its methodology was as follows:

Literature Review – ISIT reviewed the existing literature for examples of Superconducting Pulsed Power Transformers. ISIT also reviewed the current literature for research into fast High Temperature Superconducting (HTS) Switches since the Phase II MACE Demonstration Unit relies on a fast HTS Switch for its operation.

Analytical Methods – Much of our preliminary analysis focused on the fundamental physics of the MACE concept, including using standard methods for solving anticipated electromagnetic, thermal, and structural performance of a MACE device using idealized geometries.

CAD Modelling – ISIT used the CAD modelling software Autodesk Inventor 2017 to design a prototype device (“MACE Demonstration Unit”) that will be the focus of Phase II. Components of this CAD model were also used to numerically simulate electromagnetic performance of the device.

Circuit Simulation – The software package LT-Spice was used to validate initial assumptions and calculations of the MACE concept identified by analytical methods.

Numerical Simulation of idealized 2D geometries – ISIT validated its preliminary analysis of MACE’s fundamental physics using the Finite Element Analysis software package FEMCAD. Specifically, ISIT examined how high frequency AC impacted the time-varying distribution of currents within a cross-section of the annular ring structure of the SPPT and the magnetic field surrounding and penetrating the structure.

Numerical Simulation of modelled 3D geometries – A CAD model of the primary and secondary coil assembly of the MACE Demonstration Unit was imported into Maxwell 3D, a three-dimensional Finite Element Analysis Software Package. ISIT then examined time varying performance of the assembly (including, distributions of currents and fields, coupling efficiency, and device energy extraction) to validate our earlier preliminary analysis of MACE device performance.

4 TECHNICAL RESULTS

4.1 CIRCUIT SIMULATION AND EM MODELLING

4.1.1 LT-SPICE Results

Excellent coupling is achieved between the MACE multi-turn SC energy storage coil (inner conductor of coax) and the single-turn copper load coil (outer conductor of the coax) by using a coaxial conductor arrangement. Good coupling in a pulse transformer typically results in good energy transfer and extraction since there is little uncoupled magnetic field leakage energy.

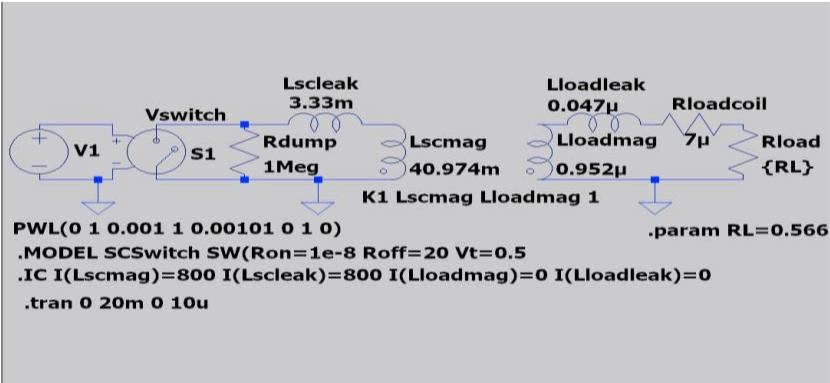
The MACE SC switch transfers energy from the SC storage coil to the load when the SC switch is quenched and driven to its OFF state. This enables the primary SC coil to be maintained in its low temperature state and only the small SC switch needs to be recooled. The voltage developed across the SC switch resistance drives a changing flux linkage in the SC coil that decreases the current; since the SC coil is magnetically coupled to the load coil, the changing flux linkage drives an increase in the current in the load coil. Because it is the total amp-turns in the coil that determines the flux linkage, the current induced single turn load coil is (ideally) N-times the initial current in the SC coil if the turns ratio is N to 1. Because of magnetic leakage flux internal to the SC coil and in the radial gap between the SC and load coil conductors, there is <100% energy transfer, but the excellent coupling of the coaxial construction helps to minimize this.

However, our circuit simulation and analysis has shown that for the SC MACE system the OFFstate resistance of the SC switch has a significant impact on the system performance.

In the OFF-state, a typical mechanical switch exhibits a resistance that is essentially infinite (unless there is a voltage breakdown), but a SC switch has an OFF-state resistance determined by the matrix or backing material used in its construction.

This SC, if used as-is in our switch, would have an OFF-state resistance of 20 Ω , so the resistance for the 188-turn storage coil that appears across the load coil terminals is $20/188^2$ or 0.566 m Ω (assuming 100% coupling and no leakage inductance). This means that the transient part of the circuit solution should be identical in its amp-turns response for both the load coil and the energy

storage coil, since both coils are connected to equivalent resistances. A simple LTSpice simulation demonstrates this.



The LTSpice circuit is shown in Figure 1, with the load resistance set to 0.566 mΩ and the SC switch OFF resistance set to 20 Ω. Inductance parameters were determined from FEMM finite element calculations based upon the circular MACE coil geometry.

Initial current in the SC coil is

Figure 1. Circuit diagram of one configuration of the MACE Demonstration set to 800 A, and the load coil current is set to 0 A.

The simulation results for the voltages and currents at both the SC coil and the load coil terminals after opening the SC switch are shown in Figure 2. Note that some quantities are scaled by the turns ratio (188) in order to properly represent them on the same scale.

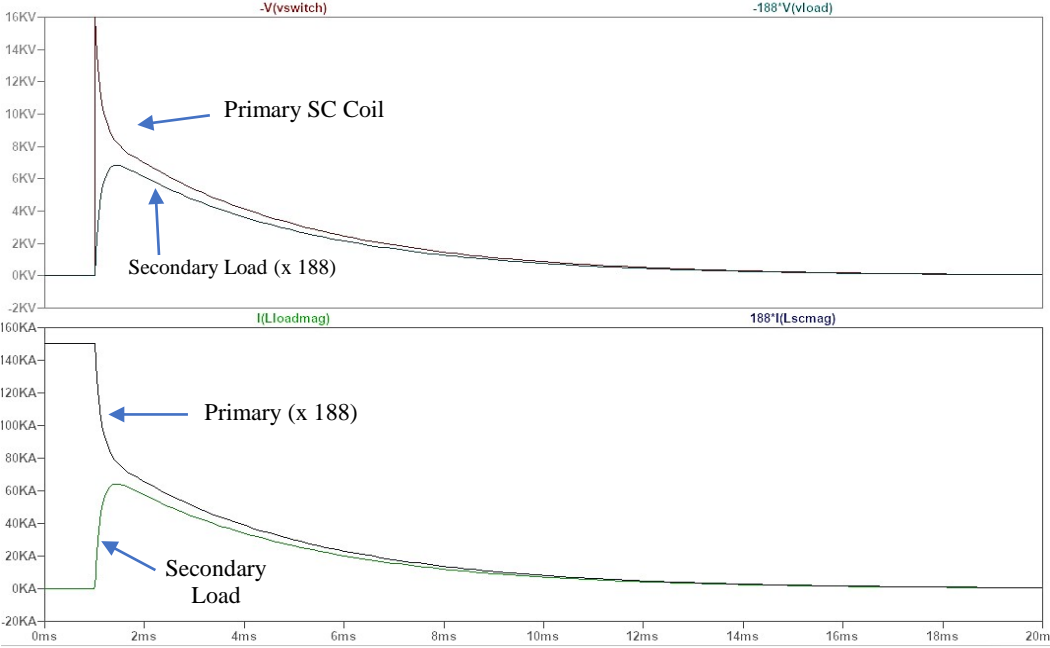


Figure 2. Simulated voltages (top panel) and currents (bottom panel) of the terminals of the SC coil and Secondary Coil

The scaled voltages and currents track almost exactly during the transient part of the curves. This case shows that nearly equal energy is delivered to the load and SC switch resistances.

Circuit theory indicates that in order to get more current (and energy) delivered to the load, the load resistance should be much smaller than the transformed switch resistance. If the load resistance is set to 0.0566 mΩ (one-tenth of the initial value), (Figure 3) the energy delivery shifts to the load and away from the switch.

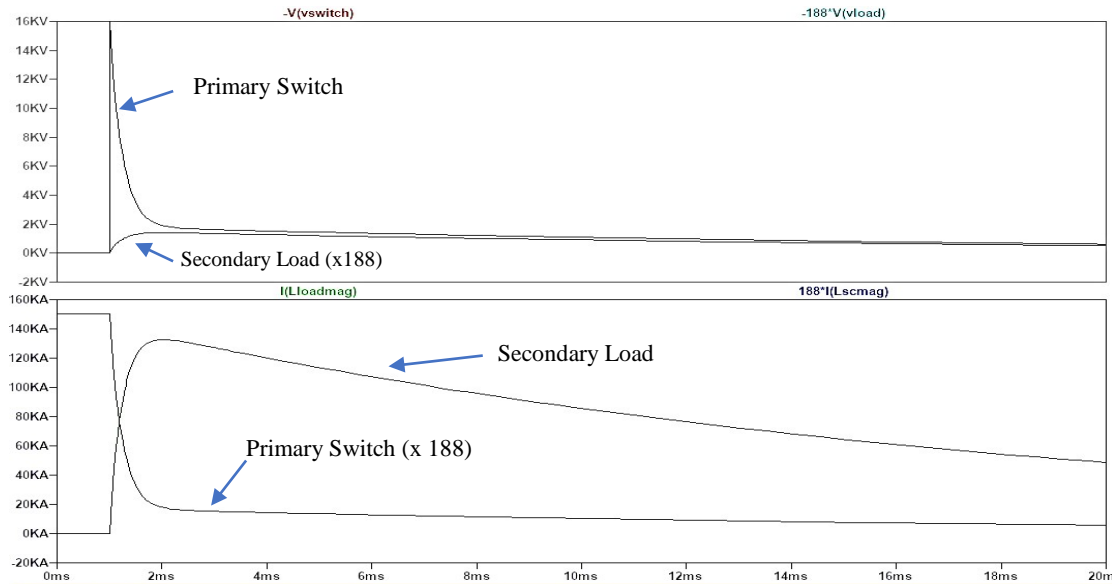


Figure 3. Simulated voltages (top panel) and currents (bottom panel) of the terminals of the SC coil and Secondary Coil when load resistance is set to 0.0566 mΩ Conversely, the load resistance is 5.66 mΩ (10 times the initial value), most of the energy is deposited in the SC switch resistance (Figure 4).

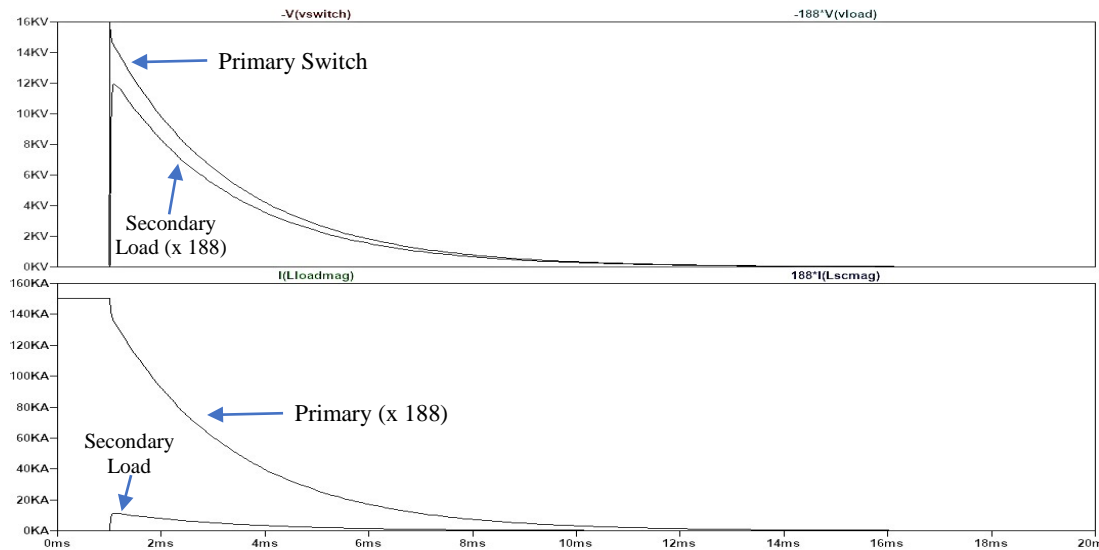


Figure 4. Simulated voltages (top panel) and currents (bottom panel) of the terminals of the SC coil and Secondary Coil when load resistance is set to 5.66 mΩ

Notice that in this circuit design, the voltage across the SC switch can never be greater than the initial superconductor current*SC switch OFF-resistance, ($800 \text{ A} * 20 \text{ } \Omega = 16 \text{ kV}$), the voltage across the load resistance can never be greater than the SC switch voltage divided by the turns ratio (in this design, $16 \text{ kV}/188 = 85 \text{ V}$).

In the switch configuration currently under study, the MACE circuit is inherently a closely-coupled air-core coil set and the currents which flow during any circuit transient are governed by the impedances seen at the terminals of each winding reflected through the turns ratio. This sets

fundamental limits on load impedance values that maximize energy transfer to the load and minimize energy deposition in the SC switch. Thus, some modification to the original electric circuit is required. Alternative arrangements for the SC switch are a topic for future research.

4.1.2 FEMM 2D FEA Results

For initial concept analysis the readily available two-dimensional finite element program FEMM is used. FEMM includes a simple geometric modeler, a triangular mesh generator, standard and user-defined material libraries, magneto-static and time-harmonic analysis engines, and a graphical post-processor.

The geometry of the MACE system lends itself to an axisymmetric model that allows one to include the three-dimensional aspect of the system in a simple way. For the purpose of this analysis, the MACE coil set has a diameter of 60 cm, the superconducting storage coil has a diameter of 3 cm, the coaxial load coil has an inner diameter that is spaced 0.1 cm from the outer diameter of the superconducting storage coil and has a thickness of 1 cm. The finite element mesh generated by FEMM is shown in Figure 5. The overall mesh contains 8626 nodes. The mesh density in the load coil conductor should be sufficient to adequately represent the skin depth behavior at 1000 Hz for analysis of coil coupling under time-harmonic excitation conditions.

Figure 6 shows the results of a magneto-static analysis for the initial charged coil state, with the expected magnetic flux density levels around the coil with 150,000 A-turns in the superconducting coil. The maximum magnetic flux density in the neighborhood of the superconducting coil is limited to approximately 2 T for the proof-of-concept experimental system; full-scale MACE

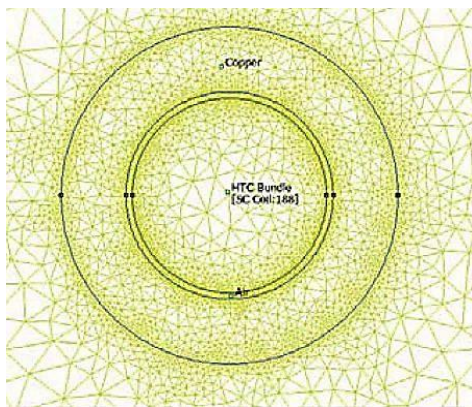


Figure 5. Finite element mesh generated by the FEMM software of the 2-D MACE model

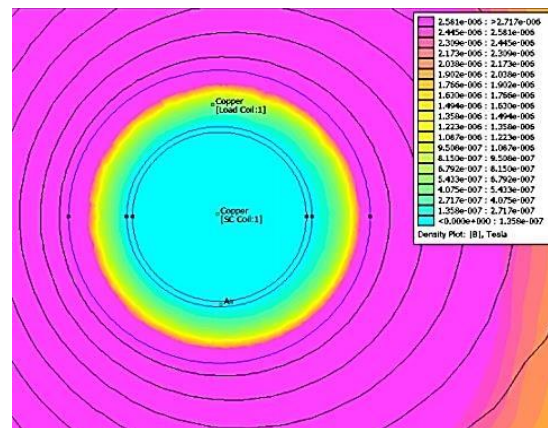


Figure 6. Expected magnetic flux density levels around the coil with 150,000 A-turns in the superconducting coil

systems are expected to utilize magnetic flux densities near 6 T or greater in order to maximize energy storage density.

In order to examine the coupling between the load coil and the storage coil, the load coil is supplied with an excitation current of 1 A at a frequency of 1000 Hz; this ensures that the skin depth of the copper in the load coil is \ll thickness of load coil conductor, which will in turn ensure that the magnetic flux density within the load coil region, where the superconducting coil is, remains close to zero. A 1-A current magnitude and assuming 1 turn for both the load and superconducting coils allows us to quickly calculate and compare inductances and mutual coupling.

Figure 7 shows the magnetic flux density plot for the time-harmonic analysis at 1000 Hz. With excitation current applied to the load coil, the magnetic flux density at the storage coil location is essentially zero due to the skin-depth behavior of the load coil conductor. Nevertheless, there is magnetic coupling between the two coils.

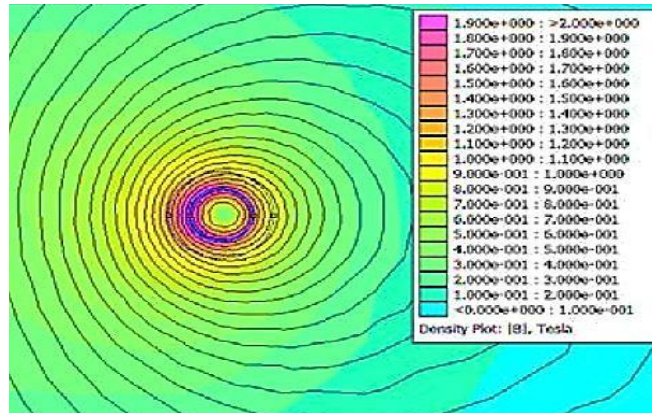


Figure 5. Magnetic flux density plot for the time-harmonic analysis of the MACE coil at 1000 Hz

The finite element analysis was used to extract circuit parameters for a SPICE simulation of the transient behavior MACE system, providing values for self, mutual, and leakage inductances.

Figure 8 shows the circuit parameters extracted using the FEMM analysis at 1000 Hz. Note that windings 2 and 3 are the two (2) halves of the load coil.

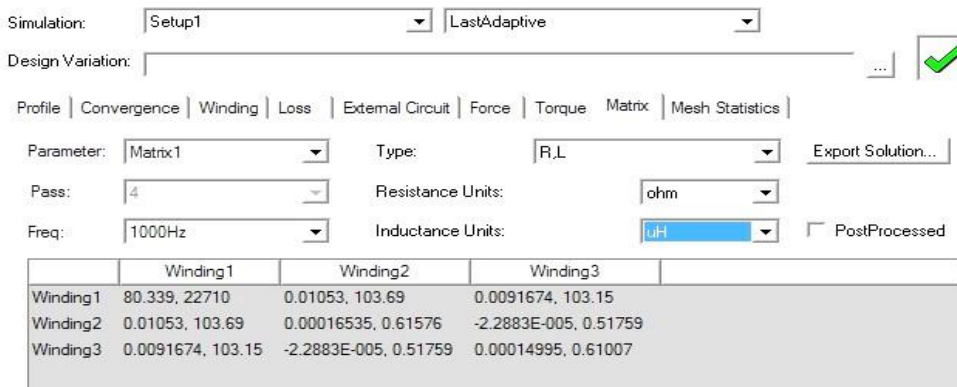


Figure 8. Circuit parameters of MACE system extracted using FEMM analysis at 1000 Hz

The non-zero off-diagonal terms of the coupling matrix in Figure 9 (below) show this coupling explicitly.

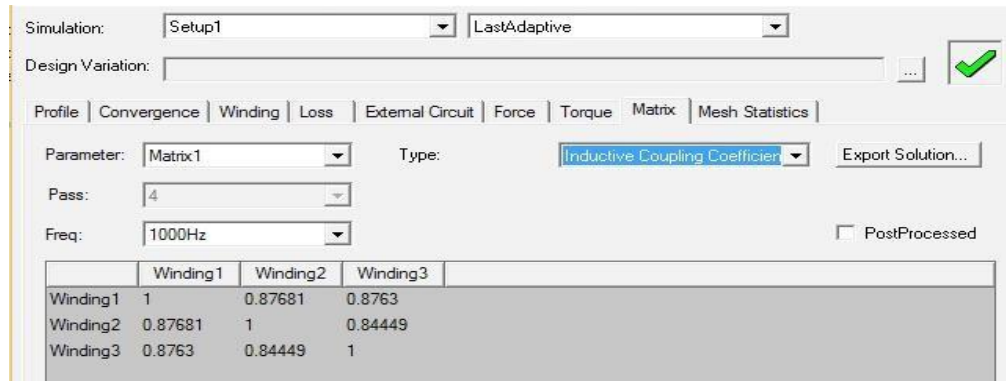
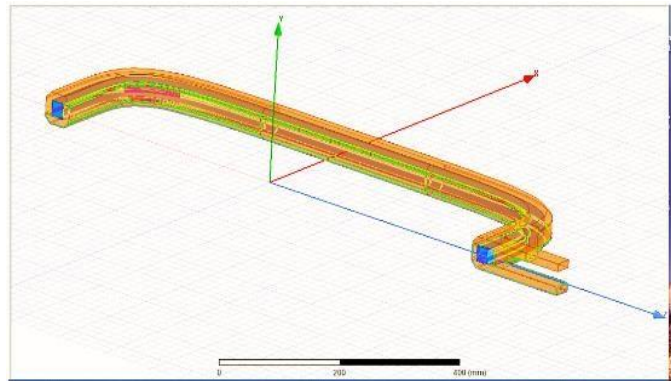


Figure 9. The non-zero off-diagonal terms of the coupling matrix demonstrate coupling between primary and secondary coils

4.1.3 Maxwell 3D FEA Results

To perform these analyses, a half-model (Figure 10) of the Inventor CAD primary/secondary coil assembly was imported into the Maxwell environment. The CAD models were modified to remove or simplify certain features like bolt holes, and to smooth some chamfer features into fillets. This was necessary to reduce the size of the FEA model and generate a proper meshing of the geometry so that the FEA solvers could function. The coil assembly



was also modelled as a half coil to further reduce the size of the FEA model. Figure 10. Geometry of the halfprimary/secondary coil assembly-

model of the MACE reduce the size of the FEA model. Because the simulation model was half-symmetry, the load coil is split into upper and lower halves; the equivalent load coil inductance is found by a reduction of the equivalent circuit for the parallel connection of both halves and is approximately $2 \times 0.6 \mu\text{H} = 1.2 \mu\text{H}$. For comparison in the LTSpice circuit simulations, the superconducting coil inductance was 44 mH and the load coil inductance was $1 \mu\text{H}$, indicating close agreement between initial closed form approximate calculations and finite element simulation results. Maxwell3D calculates coupling between the energy storage winding and the load coil is approximately 0.88. A transient finite element simulation was performed for the first 2 msec of the discharge period. The time evolution of the currents in the superconducting energy storage coil and the load coil (Figure 11) indicate that current to the external load will reach a maximum of 118 kA within the first millisecond of discharge.

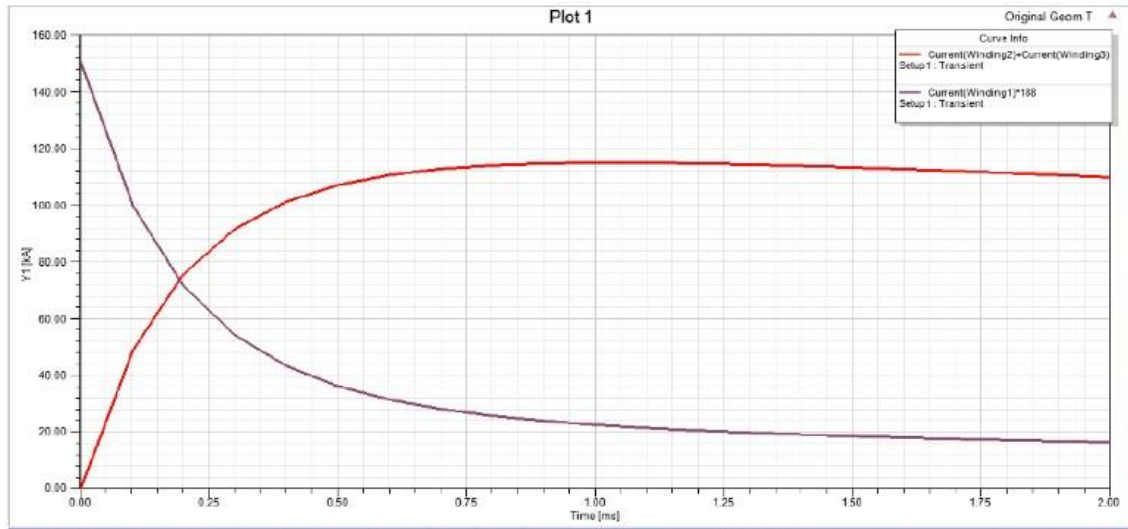


Figure 11. Time evolution of the currents in the superconducting energy storage coil and the load coil after firing

FEA Simulations of MACE Experimental Demonstrator

Standby Mode Magnetic Field: Prior to discharge, the peak magnetic flux density occurs near the corners of the superconducting coil bundle. At the surface of the HTS primary coil, ISIT saw a magnetic field strength a little above the 2 T that was originally calculated (Figure 12). Also, Maxwell3D gives the stored magnetic energy as 8.9 kJ in the half-symmetry model, so the magnetic energy stored by this coil is 17.8 kJ, very close to the design goal of 18 kJ. ISIT noted that the boundaries of the region around the model can affect the energy storage, and ISIT expected that the actual energy storage to be slightly larger.

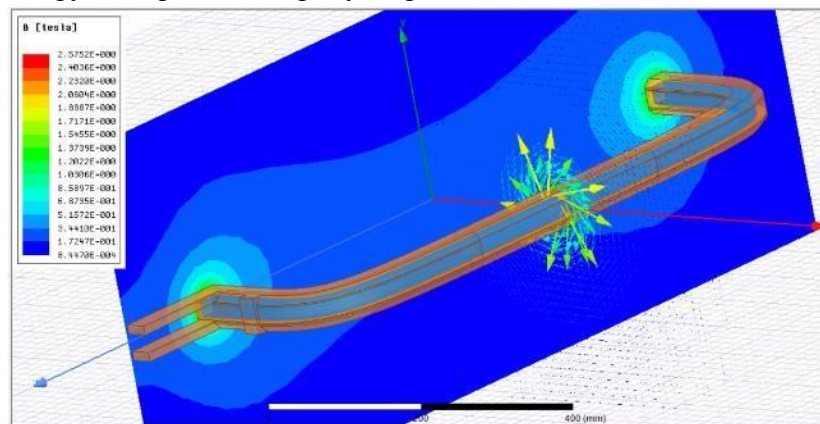


Figure 12. Steady state magnetic field simulation of MACE coil prior to discharge

Transient Behavior During Discharge: To evaluate primary to secondary coupling in the MACE system and to provide a reasonable starting mesh for the transient discharge case, an eddy current simulation was performed using a 1 kHz 800 A current in the superconducting coil. A stranded superconducting coil is assumed, while the load coil is assumed to be solid copper that will exhibit

skin effect current distribution. The load coil is assumed to be connected to a $100 \mu\Omega$ load resistance which will dominate the current magnitude induced in that winding. A color magnitude plot of the current density in the load coil winding reveals the skin effect distribution (Figure 13). The dynamic range of the plot is somewhat limited, but one can clearly see that the load connection leads on the right side support a higher current density than the main structure of the load coil. This will be addressed in the final design analysis.

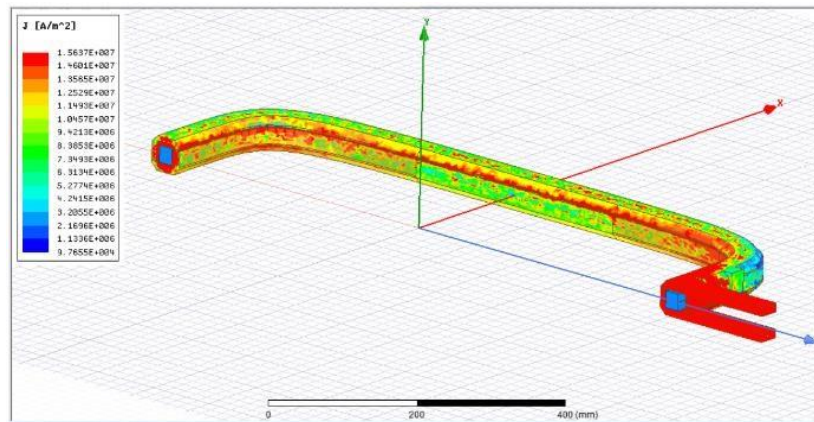


Figure 13. Skin effects of current distribution

The magnetic field distribution and current distribution was modelled at 1 msec after discharge (Figure 14). Note that the magnetic field strength has already begun to diminish as energy is transferred to the external load. The “parallel line” construction of the output leads contributes to the B field distribution in the right-hand region of the plot. The current density distribution in the output coil shows higher current density next to the superconducting coil and on the inner surface of the coil due to the eddy current redistribution. The output leads show a high current density also, as was seen in the eddy current simulations; this is primarily due to the high B field density near those leads.

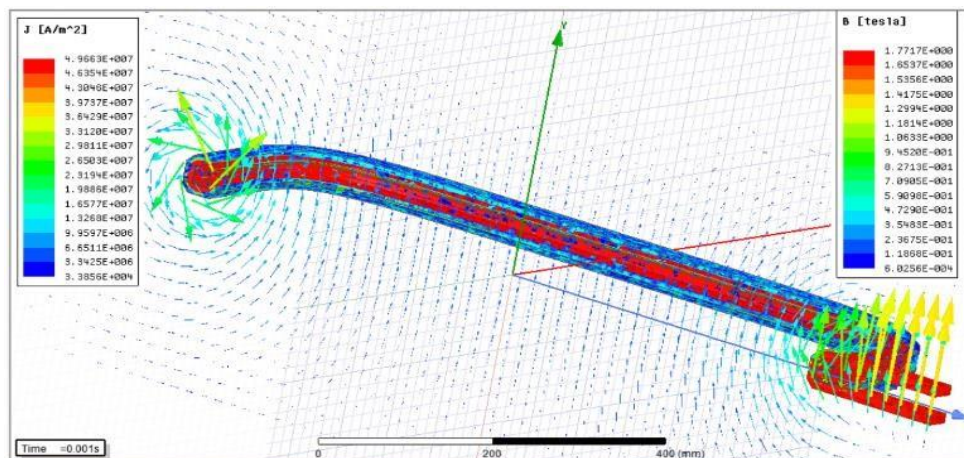


Figure 14. Transient simulation magnetic fields and skin effects at 1 msec into discharge.

These results, together with the other Maxwell3D finite element simulations described above, confirm the initial design parameters and circuit simulation results for the MACE demo coil configuration.

4.2 ENGINEERING DESIGNS

ISIT completed a full CAD model of the MACE Demonstration Unit using the Autodesk Inventor 2017 software package. Here ISIT describes an overview of the completed design and highlight some aspects of key sub-assemblies within the design. Further discussion of the requirements and design choices that led to the final design is found in Section 5.

4.2.1 Overview of MACE Demonstration Unit Design

The main function of the MACE Demonstration Unit (Figure 15) is to transfer energy from the HTS primary loop into the normal conductor secondary loop and then out to the external load. To accomplish this, several specialized sub-assemblies needed to be designed and modeled in CAD. These include:

- Primary/Secondary Loop Assembly
- HTS Switch and Dewar Assembly
- Cryocooler and Thermal Coupling Assembly
- Primary and Secondary Demountable Leads Assemblies
- Main Unit Vacuum Vessel Assembly

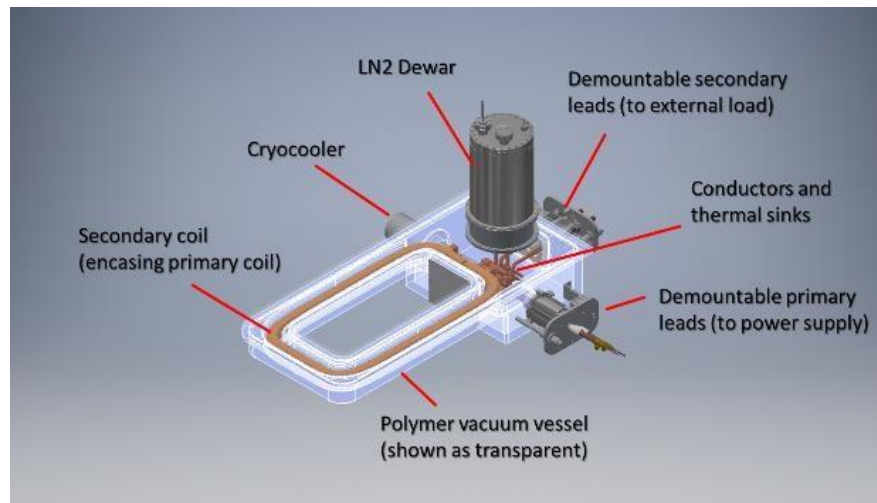


Figure 15. Main subsystems of the MACE Demonstration Unit.

4.2.2 Primary/Secondary Coil Assembly

The primary coil (Figure 16) is a 188 turn, double pancake-type high temperature superconducting coil. The primary coil is wound in a rectangular hyperellipse geometry measuring 91 cm by 25 cm. After winding, the cross-section of the completed coil measures 25-mm square. The

individual turns in the primary coil are electrically insulated from each other by 5 mils of Nomex insulation.

The secondary coil is a bipartite solid copper form, which is bolted together around the primary coil to create an annular coil that completely encloses the primary (Figure 17). The wall thickness of this shell (12.5 mm) is sufficient to allow both efficient current transport during firing, and also to withstand the hoop stresses placed on the system during operations.

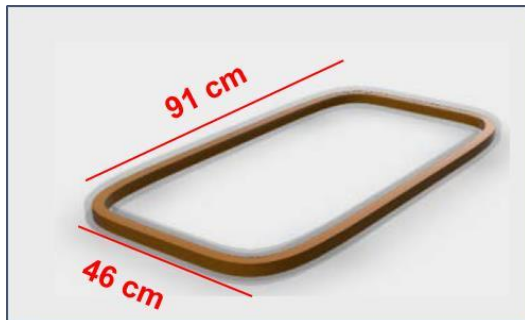


Figure 16. Geometry of the HTS primary coil. Secondary coil is shown as translucent layer encasing the primary coil

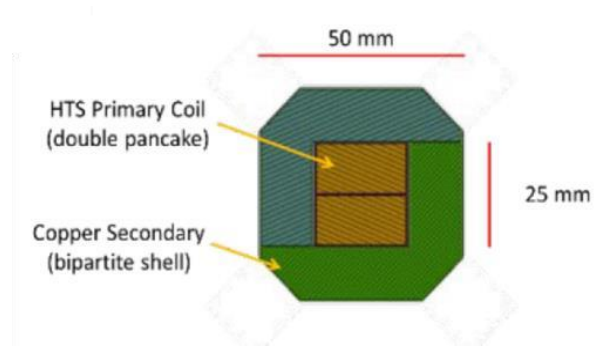


Figure 17. Bipartite shell of the secondary coil encasing the primary coil

4.2.3 HTS Switch and LN2 Dewar Assembly The HTS switch assembly (Figure 18) is designed to operate under standby conditions at subcooled LN2 temperatures (70 K). Therefore, the switch coil and its coil form is directly cooled by immersion in LN2. At the time of firing, however, the HTS switch will absorb approximately 1.9 KJ of energy, raising it above its critical temperature, and must therefore be immediately cooled back down to operating temperature. Our design uses a gravity-feed LN2 Dewar system that allows LN2 to flow through the perforated coil form quickly, carrying away heat, and thereby directly cooling the HTS switch after firing.

4.2.4 Cryocooler and Thermal Coupling

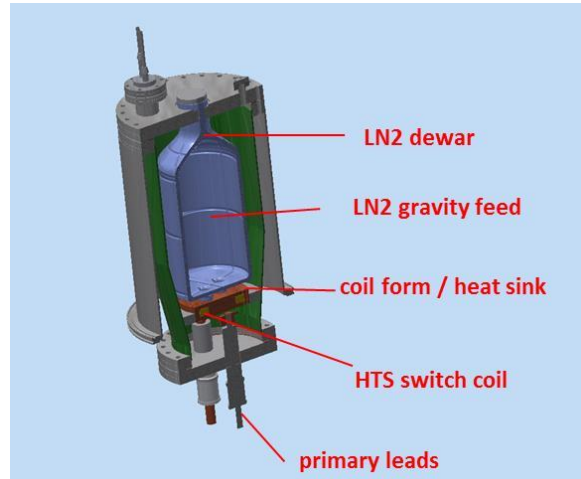


Figure 18. HTS switch assembly with major subassemblies labeled.

A major challenge in designing the MACE Demonstration Unit was to effectively cool both the primary and secondary coil circuits with a single cryocooler. Additionally, all three (3) assemblies (the primary circuit, the secondary circuit, and the cryocooler), as shown in Figure 19, needed to be thermally coupled but remain electrically isolated from each other due to high voltages that can occur during triggering. The final design overcame these challenges by including a Nomex electrical insulation layer between the mated connections of the copper circuit assemblies to the copper cold head of the cryocooler. The Nomex is thin enough (5 mils) to readily allow rapid cooling of the circuits by the cold head, but also electrically insulate the assemblies from each other.

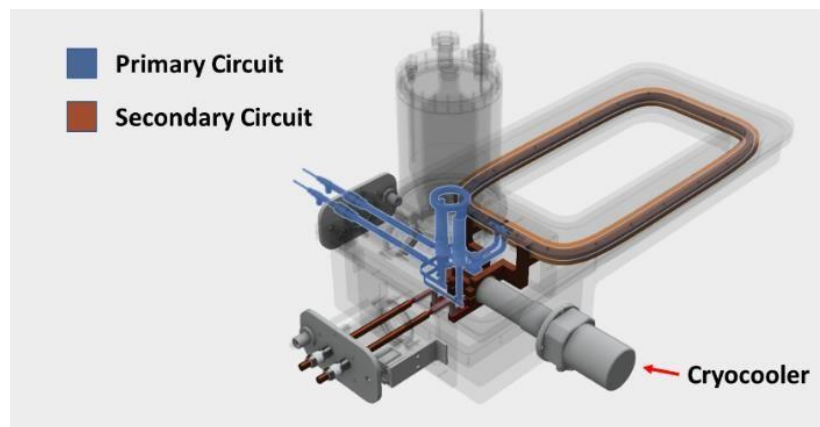


Figure 19. Thermal coupling of cryocooler with both the primary and secondary circuits

4.2.5 Demountable Leads

Another challenge in designing the MACE Demonstration Unit was the prevention of heat loss to the exterior via the electrical leads. During standby operation, prior to triggering, the use of large diameter, permanently connected external leads would lead to unacceptable heat losses due to the

high thermal conductivity of copper. A solution was found such that both the primary and secondary external leads could be coupled or decoupled (“demounted”) from the internal leads, within a matter of seconds. The design (Figures 20 and 21) incorporates the use of an expandable metal vacuum bellows that can be pushed into place to connect the external leads to the internal leads at a bullet-type mounting point. Disconnection is accomplished by pulling the bellows assembly away from the vacuum vessel.

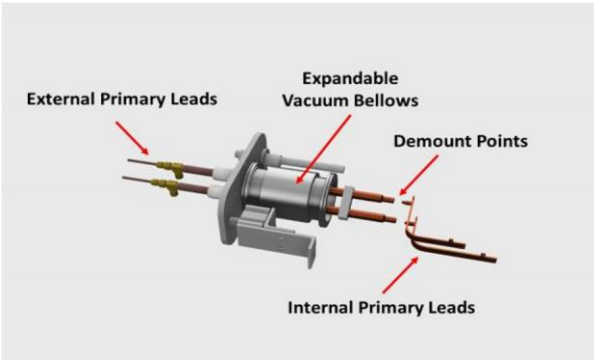


Figure 20. Demountable lead system for the primary circuit

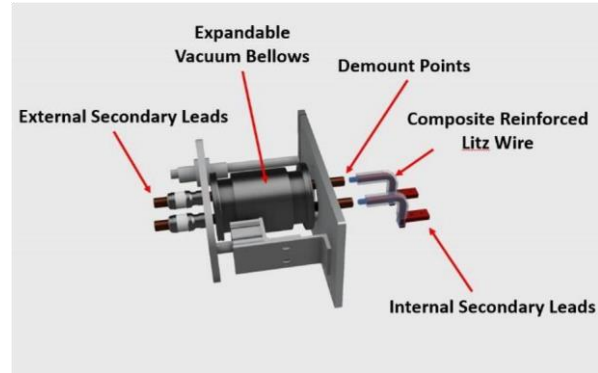


Figure 21. Demountable lead system for the secondary circuit

4.2.6 Main Unit Vacuum Vessel

The main vessel enclosing the primary/secondary coil assembly as well as the cold head and thermal/electrical coupling system must fulfill two criteria. First, it must be made of a non-metallic material in order to minimize inductive coupling-related losses in the primary/secondary coil during operation. Second, it must be sufficiently rigid to withstand the stresses created when the interior is held in a vacuum. The chosen solution (Figure 22) is to mill the main unit pressure vessel from a solid block of High Density Polyethylene (HDPE).

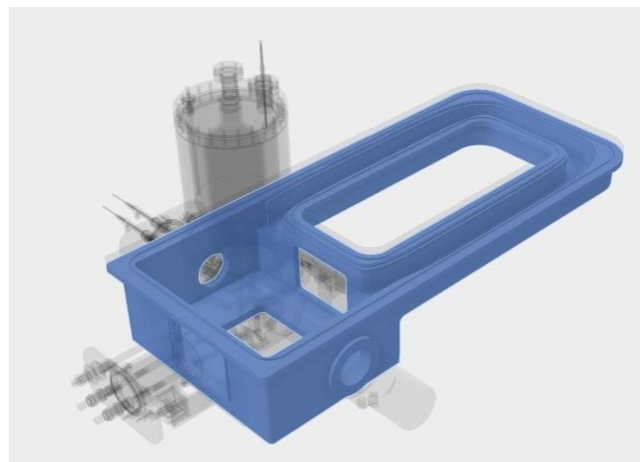


Figure 22. Main Pressure Vessel of the MACE Demonstration Unit

5 IMPORTANT FINDINGS AND CONCLUSIONS

5.1 MILITARY RATIONALE

Potential Military Applications of MACE Superconducting Pulsed Transformer

The Department of Defense (DoD), Department of Energy (DoE), NASA and the military services have invested large amounts of funding for decades to find compact electrical pulsed power sources for a variety of applications. In the 1980s, the Defense Nuclear Agency (DNA) successfully developed high energy and high power density capacitors for nuclear simulators and other military applications.

As this technology was being developed and commercialized, these capacitors were combined with the necessary switches and safety devices to create Pulsed Forming Networks (PFNs) to enable electrical pulses to be created with a variety of voltage and currents. The capacitor PFNs have become the standard for laboratory and other pulsed power applications. For example, they have been used extensively as power sources for directed energy and electromagnetic launch systems (such as Railguns).

Unfortunately, the capacitor-based PFNs are too large and heavy for most mobile military systems, but since they are reliable and available commercially, they have been used extensively in all pulsed power laboratory facilities. For example, the Navy accumulated large PFNs to power their laboratory railguns and decided to go forward with ship-based capacitor PFNs since they had sufficient space on board their large naval platforms. In parallel, they continued to develop higher energy density PFNs for ultimate ship-board use. A standard sea-container (38 m³) in 2010 was able to hold a capacitor PFN storing 8 MJ. The Navy has continued to fund industry to develop advanced capacitors and novel packaging so that the state-of-the-art has been increased from the ability to store 8 MJ to now 15 MJ in the same size sea-container. This is the result of much expert technical effort and is probably about the energy density limit for capacitor PFNs unless there is some unforeseen technical breakthrough in advanced capacitor materials.

In the 1980s, OSD initiated the National Electromagnetic Launch Technology Program (EML) and the Army took the lead in investigating high-energy-density pulsed alternators (compulsators) as the potential power supply for mobile EML systems. However, after an investment of several hundred million dollars over 30 years, the Army declared in 2010 that they did not have a power supply solution for a mobile railgun and cancelled their pulsed power and railgun programs.

An understanding of the fundamental physics behind these limitations can be seen in Figure 23:

Why Superconductor Inductive Storage?



- provides best combination of energy density, cost per MJ, and system reliability

Device	Storage Mechanism	Defining Equation	Assumption	Limiting Values	Theoretical Energy Density (MJ/m ³)	Real World Energy Density (MJ/m ³)
Capacitor	Electrostatic	$E = \frac{CV^2}{2}$	High energy density plastic film	$E_{app} = \frac{400V}{\mu m}$ $\epsilon_r = 3.5$	5	0.9-1.2 (GA)
Rotor (Pulsed Alternator)	Inertial	$E = \frac{I_m \omega^2}{2}$	High speed composite / conductor rotor	$\rho = 1,500 \text{ kg/m}^3$ $V_{rotor} = 600 \text{ m/s}$ (COMPLEXITY)	135	0.8 (CEM)
Inductor	Magnetic	$E = \frac{B^2}{2\mu_r \mu_0}$	High field air-cored inductor	$\mu_r = 1$ $B = 10-15 \text{ T}$	150	10-20 MACE-TBD
Battery	Electrochemical		LIMS	1.72 V	4,000	0.9 (Tesla)

ISIT Proprietary Information

Figure 23. Principle of operation and fundamental limits for various energy storage technologies.

Electrical energy can be stored electrostatically in capacitors, inertially in the rotors of pulsed alternators, magnetically in inductors and electrochemically in batteries. It is obvious from the chart that the theoretical energy density of batteries is orders of magnitude higher than capacitors, but the internal resistance prohibits the energy from being extracted rapidly for pulsed power applications. Pulsed alternators potentially can achieve much higher energy and power density than capacitors but the complexity and necessary high rotating speeds have not led to a successful solution to date. Inductive storage is an attractive alternative, but the resistive losses have precluded a practical solution, until now. Advances in high temperature superconductors and their commercial availability as a result in the proliferation of medical magnetic resonance imaging machines have now enabled superconducting inductors to be serious candidates for compact pulsed power sources. The MACE superconducting pulsed transformer will provide an order of magnitude increase in energy and power density over the capacitor PFNs enabling significant reduction in size of the Navy power supply for their 32 MJ ship-based railgun and may enable MOBILE military systems for all of the military services.

Shown below (Figure 24) are current high-energy LASER, high-power microwave and the General Atomics Blitzer Railgun and their capacitor PFN power supplies. The SC pulsed transformer will enable similar systems to be constructed with much less volume and weight.

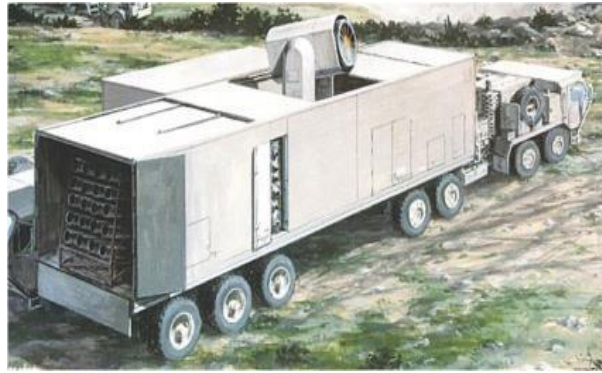


Figure 24. Current Directed Energy and Rail Gun Systems in development that could benefit from SC pulsed power transformers.

Thus, the MACE SC pulsed transformer can significantly reduce the size of electric weapons systems and could enable **mobile** military systems for a broad class of directed energy (high-power microwave, LASER and EM launcher) weapons systems and they could replace capacitors as the power source for a number of other important military pulsed power applications.

5.2 DESIGN REQUIREMENTS OF MACE DEMONSTRATION UNIT

5.2.1 Primary Coil Design

Choice of Superconductor: The most important requirement of the MACE primary coil is to generate as strong a stable magnetic field as possible without losing any energy to resistive losses during the energy storage or “charged” phase of MACE operation. Therefore, MACE requires a High Temperature Superconductor (HTS) that exhibits excellent critical current capacity (I_c) while exposed to high magnetic fields. Second generation HTS tapes using YBCO superconductors commercially-available from Superpower Inc. (Schenectady, New York) have an I_c of approximately 1500 A per 12 mm width when operating at 30 K and 2 Tesla magnetic field, or almost double the likely design requirement for the MACE Demonstration Unit (Option 1).

Superpower's HTS product appears to offer the best combination of I_c , in-field performance, mechanical strength, overall tape thickness, long piece lengths, and price.

Operating Temperatures: As with all HTS tapes, critical current increases with decreasing temperature (Figure 25). Thus, it is possible to generate the same strength magnetic field using less HTS tape if MACE is operated at lower temperatures. The main trade when determining MACE operating temperature is the cost and complexity of the cryogenic system versus the cost savings of using less HTS at lower temperatures. A liquid helium-cooled system (4 K) would offer far greater magnetic energy storage per unit volume than a liquid nitrogen cooled system (77 K), but at greater cost and

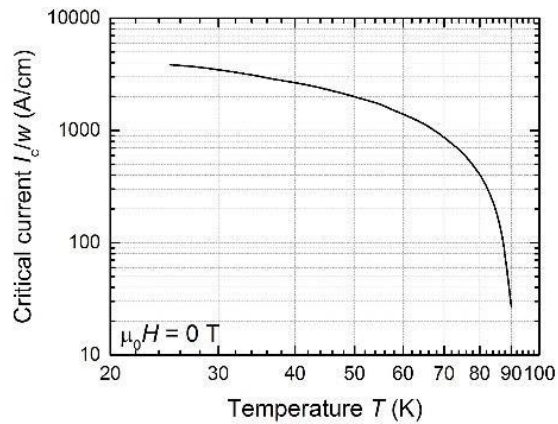


Figure 25. Temperature dependence of I_c in HTS Tape.

reduced system reliability. It appears that a MACE unit operating at 30K would increase I_c in ^{source:}

the HTS tape by 3-fold over liquid nitrogen <https://doi.org/10.6084/m9.figshare.3759321.v1> temperatures. A 30K system would also allow cryogen-free, conduction-based cooling of the primary coil using standard commercially-available cryocoolers.

Choice of Geometry: An important goal of the next phase (“Option 1”) of the MACE program is to demonstrate efficient transfer of stored energy from the MACE coil to an external load within 10 msec or less. There are several different coil geometries that could accomplish this goal, including circular coils, square coils, and rectangular coils. From a fabrication viewpoint, a circular coil would provide the simplest form to build while also minimizing the amount of required HTS. However, in designing MACE for its final field-deployable form, a rectangular coil is ultimately preferable since MACE will ultimately use a toroid geometry to minimize stray fields that could impact personnel and sensitive equipment. Compared with circular and square cross-sections, toroids with rectangular cross-sections offer the best combination of volumetric energy density, form factor design freedom, and economy of required HTS (Figure 26).

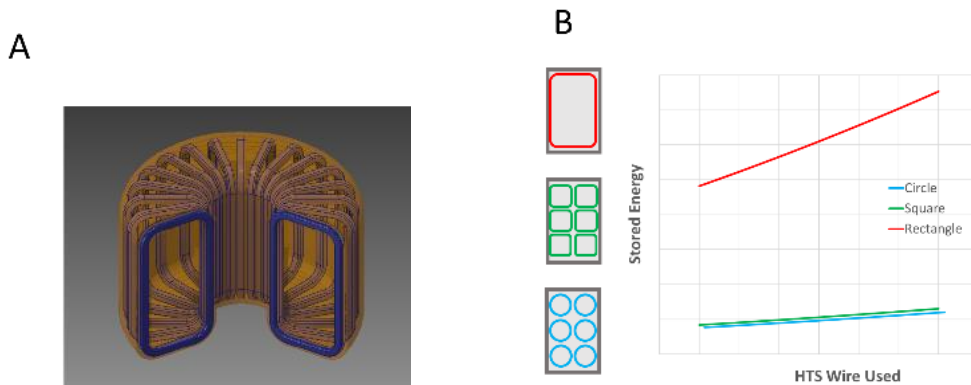


Figure 26. Loop geometry choices for MACE. While a circular or square geometry might be most efficient for a single primary coil, when multiple units are integrated into a toroidal form, rectangular loops offer more stored energy for an equivalent length of HTS.

5.2.2 Secondary Coil Design

Operating Principle of the Annular Shell Design: The MACE secondary coil is a single turn coil that multiplies the current flowing to an external load by a factor proportional to the turns in the primary coil. To maximize energy transfer efficiency, the secondary coil in the MACE concept is designed as an annular shell (Figure 27) that completely encloses the HTS primary coil to capture energy stored in magnetic field surrounding the primary coil when the MACE device is triggered. An additional advantage of the annular shell design is that for the purposes of the MACE Demonstration Unit, a metal secondary coil is robust enough to provide full structural support for the primary coil, restraining it from hoop stresses while operational.

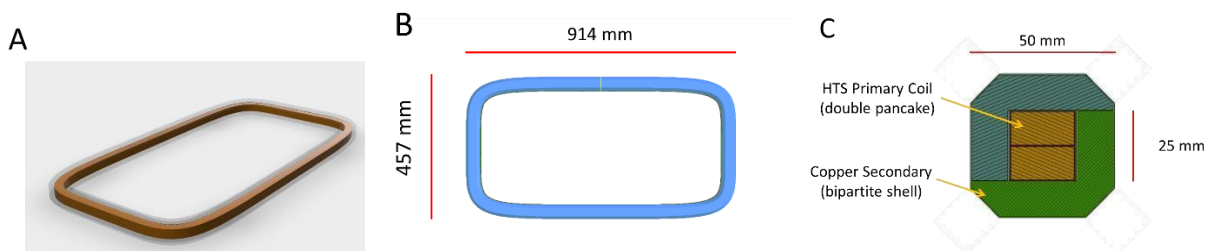


Figure 27. Preliminary design of the MACE Demonstrator Unit primary and secondary coil
 (A) CAD rendering of the HTS primary coil embedded within the transparent secondary shell.
 (B) Dimensions of the MACE secondary shell.
 (C) Cross section view of the coils.

Choice of Material: The secondary coil must provide a combination of low resistivity (to maximize energy transfer), low magnetoresistance (to minimize changing electrical conductivity in changing fields), high thermal conductivity (to enable rapid cooling), with good structural characteristics (to restrain the primary coil). The two obvious candidates for material are copper and aluminum. Copper is traditionally used when constructing coil forms for superconducting

magnets for small to medium size magnets since copper presents superior characteristics, especially at cryogenic temperatures, and is also less susceptible to oxide layer formation which can inhibit electrical and thermal conductivity. Aluminum may be used in the case of very large magnets to reduce overall weight. For the MACE Demonstration Unit, copper is the clear material of choice for the secondary coil.

Solid vs Litz Wire Shell: Initially, it was believed that the energy contained in the collapsing magnetic field would best be captured by a annular secondary coil made from Litz wire. In this application, it was believed that the use of Litz wire would reduce the skin effect exhibited in the secondary coil and thus reduce ohmic losses as the current was transferred to an external load. However, preliminary calculations indicate that a solid shell is sufficient for the MACE Demonstration Unit. The solid shell option also provides the needed structural support, and is easier to fabricate.

Operating Temperature: Unlike the HTS primary coil, which must operate at cryogenic temperatures to maintain superconductivity, the secondary coil could operate at ambient temperatures and still transfer current to the external load. However, operating the secondary coil at either 30 K (the temperature of the primary coil) or 70 K (the temperature of subcooled liquid nitrogen) presents numerous advantages, including lower overall electrical resistance and lower temperature differentials between primary and secondary (enabling more efficient cooling of the primary and simpler thermal insulation structures). In Phase II, the MACE Demonstration Unit, the cooling of the primary coil will be achieved via conduction cooling of the secondary coil physically coupled to a cryocooler cold head. Thus, for the demo unit, the operating temperature of the secondary coil will be 30 K. However, for the subsequent Phase III (the MACE Field Unit prototype), the power dissipation in the secondary is anticipated to be 1000-X higher, leading to much larger resistive heating in the secondary. In this case, the secondary will likely be directly cooled with liquid nitrogen subcooled to 70 K.

5.2.3 Preferred Design and Operating Characteristics for MACE Demonstration Unit

For the MACE Demonstration Unit (Figure 27), ISIT anticipates building a rectangular primary coil and an encasing secondary coil with the specifications listed in Table 1.

Table 1. Preliminary Specifications of the MACE Demonstration Unit

• 150,000 A turns in primary SC winding	• 1.71×10^{-6} H equivalent single-turn external inductance, L_{ext}
• 2 T magnetic field strength at surface of SC winding	• 19.2 kJ external magnetic energy, E_{ext}
• 30 K operating temperature	• 1.3×10^{-6} H equivalent single-turn internal inductance, L_{in}
• 1.2 cm wide YBCO high temperature superconductor (HTS) tape	• 1.5 kJ internal magnetic energy of MACE coil, E_{int}
• 1500 A critical current of HTS tape at 30 K and 2 T	• 7.8% of total energy is internal magnetic energy, E_{int}/E_{TOT}
• 800 A operating current in tape	• 3 msec discharge time
• 188 turns of HTS tape	• 6.4 MW average discharge power to external load
• 490 m total tape length	• 150,000 A initial discharge current to external load

5.3 SWITCHING

5.3.1 Requirements for the MACE high temperature superconducting switch

A primary function of the MACE HTS switch is to enable the rapid draining of current flowing in the primary coil so that energy stored in the magnetic field can be transferred to an external load. The HTS switch therefore must meet certain key requirements:

- Negligible “ON” resistance / relatively large “OFF” resistance
- Fast Switching Speeds
- Robust
- Rapid cycling

Switch Resistance: A high “OFF” resistance in the HTS switch accomplishes two objectives. First, it minimizes the coupling losses between the primary and secondary coils by maximizing the impedance ratio between the primary circuit loop and the secondary circuit loop. Thus, a high impedance ratio ensures that energy can be transferred quickly and efficiently to the external load. Second, a high “OFF” resistance permits current flowing in the primary circuit to be effectively dissipated either through resistive losses through the switch itself, or by shunting the current to an auxiliary dump resistor whose resistance, while lower than the “OFF” HTS switch, is still large enough to dissipate the primary circuit current quickly.

For the MACE Demonstration Unit, ISIT has calculated that ISIT will require an HTS switch with an OFF resistance of at least $20\ \Omega$ in order to drain most of the primary circuit current in under 10 msec while also maintaining an efficiency of energy transfer to the external load of greater than 90%. ISIT believes it is possible to achieve this required OFF resistance by fabricating a HTS switch that is comprised of 10 m of “stabilizer-free” 12-mm wide HTS tape. The term “stabilizer free” means that the copper jacket that usually encases the HTS tape is not present, and therefore the HTS tape does not have an alternate low resistance pathway for the current to flow when the YBCO superconductor is transitioned to normal. Reported resistance (while in the normal conducting state) for our HTS tape of choice for this component is $2\ \Omega$ /m of length.

Fast Switching Speeds: The switching speed of HTS switches is ultimately determined by the speed of quenching, i.e. how fast the superconducting material in the switch can transition from a superconducting state to non-superconducting state. During the quench process, a region of the HTS material will suddenly transition to a state where the current (I) flowing through the material is greater than it’s rated critical current (I_c). The critical current is the maximum current the HTS material can handle at a given temperature and magnetic field before the material transitions to a normal conducting state. Methods of initiating quench can include,

- 1) injecting additional current into the circuit,
- 2) thermally heating the HTS tape, or
- 3) exposing the HTS tape to an increased ambient magnetic field.

Most research into HTS switches thus far have focused on method 2, thermally heating the HTS tape so that its I_c threshold is lowered and quench is initiated. However, the main objections to the

heating method are that it is relatively slow and can possibly damage the HTS tapes after repeated direct heating.

A better method is described by Solovyov and Li (2013) in which they use a high-frequency RF field to drive the HTS tape normal over a relatively large area in a short time period. In this approach, an RF coil is interleaved between two sections of HTS tape (Figure 28) such that the energized RF coil (100 kHz) induces additional currents within the HTS tape such that $I > I_c$ and the switch is driven normal. One advantage of this method is that the HTS tape can be uniformly driven normal very quickly (<5 msec) over a comparatively large area of tape (e.g. from 10s to 1000s of

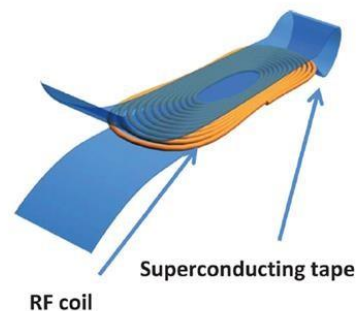


Figure 28. A fast HTS switch using a coupled RF field to induce quench.

square centimeters of tape). Our preliminary switch design consists of 10 m of HTS tape (i.e. >1,000 cm² of HTS tape) *source: Solovyov and Li, 2013* wound into a non-inductive bifilar coil (e.g., a coil that is wound in a way not to generate its own magnetic field). Interleaved between the HTS tape layers in the bifilar coil, a custom 5-m long RF coil tape will be interwound to trigger quenching in as little as 2 msec.

Robust and Reliable Operation: Ideally, the MACE HTS Switch should operate 1000s of times over a period of years. This means that the HTS material must endure 1000s of quench cycles, each with its own period of resistive heating followed by cooling and renewed superconductivity. Early research into quenching of HTS coils indicated that HTS tapes could be easily damaged by quench/cool cycles. A common failure mode was found to be the delamination of the YBCO layer that occurred post-quench during rapid re-cooling with liquid nitrogen (LN₂). However, further study (Takematsu, et al., 2010), indicated that delamination of the fragile YBCO layer occurred during rapid cooling not because of the material properties of the YBCO layer itself, but because the HTS coil itself was constructed using an epoxy impregnation technique to add structural strength. When the epoxied coil was rapidly heated and cooled, the epoxy layers bonded to the tape would literally pull layers off the tape. Furthermore, it was discovered that when HTS coils were either dry-wound or impregnated with weakly adhesive paraffin (instead of epoxy) the HTS coils showed no failure or delamination of the YBCO layer even after multiple rapid cycles of heating and cooling. As the CAD design of the MACE HTS Switch progresses, a key design requirement will be to wind and support the bifilar coil with a method that that minimizes mechanical stress experienced by the HTS tape during operation while also allowing the surrounding LN₂ to transfer heat away from the switch as quickly as possible.

Rapid Cycling: Based on our calculations for a preliminary HTS switch design, ISIT believes the MACE HTS switch itself will be able to fire, cool, and be reset for subsequent firings in under 1 second. The cycling time of the entire MACE Demonstration Unit will be somewhat longer since it will also depend on other factors such as charging time, telemetry gathering, safety checks, etc.

During firing, the MACE HTS switch will need to dissipate approximately 1.3 kJ of energy in under 10 msec, for an average power dissipation of 130 KW. The MACE HTS switch itself will be immersed in liquid nitrogen (LN₂) that is sub-cooled to 70 K. Thus, a small amount of LN₂

will be vaporized with each firing of the unit. Since LN2 has a heat of vaporization of 5.56 kJ per mole (160,128 J/L), MACE Demonstration Unit will ultimately vaporize approximately 8 mL of LN2 per firing event.

The heat generated within the switch during firing will initially increase its temperature by approximately 75 K, since the heat cannot be transferred instantaneously to the LN2. The switch region comprises approximately 1000 cm² of HTS tape surface area that is in contact with the LN2. The maximum heat flux possible with LN2 is about 10 W/cm². Thus, across its entire surface area, the HTS switch can transfer heat at 10,000 W, and the time required to remove the heat from the switch will be 1,300 J /10,000 J/sec, or 0.13 sec.

References:

Solovyov, Vyacheslav F., and Qiang Li. "Fast high-temperature superconductor switch for high current applications." *Applied Physics Letters* 103.3 (2013): 032603.

Takematsu, T., et al. "Degradation of the performance of a YBCO-coated conductor double pancake coil due to epoxy impregnation." *Physica C: Superconductivity and its applications* 470.17 (2010): 674-677.

5.3.2 Requirements for the Dump Resistor

Our initial MACE concept included a “dump resistor” designed to carry most of the current during MACE firing, and thereby. However, this initial concept has been refined. At modest energy storage levels, as will be shown in the MACE Demonstration unit, the HTS Switch itself is able to dissipate the energy contained in the primary coil. Adding a dump resistor in parallel with the HTS switch would simply act to lower the overall resistance of the circuit thereby lowering the impedance ratio and efficiency of energy transfer. Since the experimental objectives of the MACE Demonstration Unit focus on the devices efficiency of energy transfer and the ability to rapidly cycle the device between charging, firing, and recharging, the use of a dump resistor for the Demonstration Unit is not warranted.

However, one of the important outcomes of the present study is the recognition that the HTS switches for the field-scale units (i.e. 10 MJ of energy storage and larger) will require a modified approach. First, to maintain high impedance ratios between the primary loop circuit and the secondary loop circuit, the HTS switch will require significantly higher “OFF” resistance than that which is required by the MACE Demonstration Unit. Another issue is that higher “OFF” resistances when combined with high turn ratios between the primary and secondary coils will generate large and potentially damaging voltage spikes at the HTS switch at the time of triggering. For these reasons, ISIT has begun to look at several modified HTS switch designs for scaled-up versions of MACE. These will be addressed in future monthly reports.

5.3.3 Requirements for Electrical Leads and Power Supply

For the MACE Demonstration Unit, the primary HTS coil winding will be charged to carry 800 amps. ISIT has identified commercial off-the-shelf demountable leads which are rated for 1000 A.

The charging power supply requirements for the MACE Demonstration Unit are modest. If charging ramp rates for the MACE primary coil are kept to a conservative 20 A/sec or less (or, 40

second coil recharging time), the charging voltage for the power supply will be $V = L \frac{dI}{dt}$, where L is the primary coil inductance (4×10^{-2} H), or 0.8 V at 20 A.

5.4 THERMAL ANALYSIS

5.4.1 Categories of thermal loads The thermal management of the MACE Demonstration Unit must contend with a number of thermal loads. Some thermal loads are constant, or “steady state” loads, whereas other thermal loads are transient and involve heating of conductors during the triggering of the MACE Experimental Demonstrator. These various thermal loads are depicted as a schematic in Figure 29.

With steady state thermal loads, there is a constant heat flux into the device across

insulation layers which must be actively cooled by the cryogenic system. These steady state loads include:

- 1) heat flux from the 300 K ambient

temperature outside the Unit into the 30 K compartment of the MACE Experimental Demonstrator;

- 2) heat flux across the primary leads from the 77K (70K) liquid nitrogen Dewar to the 30 K compartment; and
- 3) heat flux across the secondary leads from the 300 K exterior to the 30 K compartment.

The transient thermal loads occur during device triggering and are related to resistive heating of normal (non-superconducting) conductors as current passes through the device. These transient thermal loads include:

- 1) I^2R heating of the secondary coil during firing;
- 2) I^2R heating of the secondary current leads during firing; and
- 3) heating of the quenched HTS switch in the 70 K compartment during firing.

5.4.2 Temperature Specification and Operating Characteristics of MACE Demonstration Unit Determine Cryogenic Approach

Choice of thermal design, including insulation strategy and cryogenic components is largely determined by the operating temperature of the primary and secondary coils of the MACE Demonstration Unit. Because the primary coil must operate at 30 K, far below liquid nitrogen temperatures, the logical approach to cooling is to use conduction cooling from the cold head of a

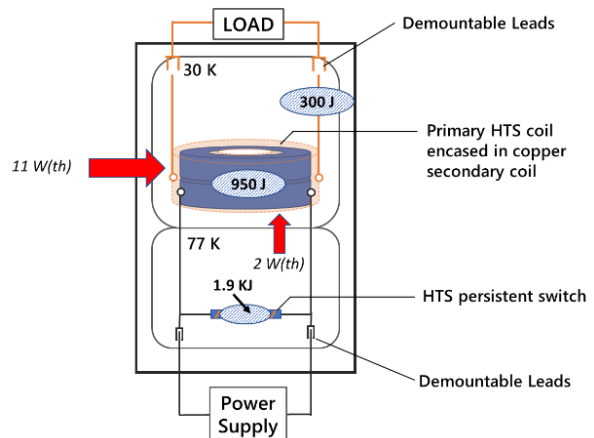


Figure 29. Schematic representation various heat loads of the MACE Experimental Demonstrator. Steady-state loads that represent constant heat flux into the device are depicted as red arrows. Transient heating of specific components that occurs during device firing are depicted as blue ovals.

cryocooler. For the purposes of making a lab-scale prototype, conduction cooling is simpler, cheaper, and more robust compared to other options such as liquid helium-based cooling.

Furthermore, because the MACE Demonstration Unit generates a magnetic field of approximately 2 Tesla, which is significantly lower than the expected MACE Field Prototype, it is impossible to maintain an insulated gap between the primary coil (which must operate at 30 K) and the annular secondary coil without significantly impacting overall energy transfer efficiency. At higher field strengths, such as are expected in the MACE Field Prototype, a 1-2 cm insulated gap will not significantly impair device efficiency. Thus, both the primary and secondary coils in the MACE Demonstration Unit must be maintained at 30 K, despite the secondary coil being subject to steady state and transient loads which could easily be cooled with liquid nitrogen. Paradoxically, perhaps, MACE becomes easier to cool as it scales up from the Experimental Demonstrator to the Field Prototype.

5.4.3 Thermal Design of Main Vessel

Because MACE is a superconducting Pulsed Power Transformer, it is important to minimize the presence of metal structural elements which could inductively couple to the primary and secondary coils. This design consideration limits the use of metal to create the main vacuum vessel (aka the 30 K compartment), the use of metal to create metallic standoffs to position the coil within the vessel, and even the use of standard thermal design elements such as metallic thermal shielding. Figure 30 shows the basic design of the main vessel, which consists of an evacuated HDPE plastic vessel that contains the main MACE coils (primary and secondary), the cryocooler cold head, and associated copper heat sink. Also shown is the liquid nitrogen Dewar that contains the HTS switch. The main MACE coils (primary and secondary) are supported in a packed bed of evacuated perlite thermal insulation (in a 2-cm width layer) which provides both thermal insulation and structural support during operations. Evacuated perlite has a thermal conductivity of $1 \times 10^{-3} \text{ W K}^{-1} \text{ m}^{-1}$ and a packed bed compressive strength of 80 psi, or well in excess of the 20-psi outwards hoop stress expected during operation of the coil.

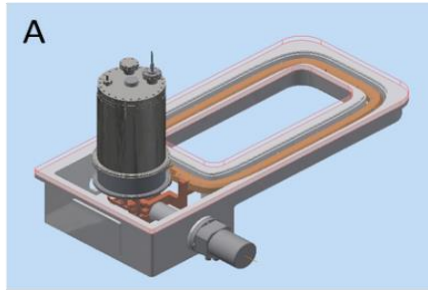
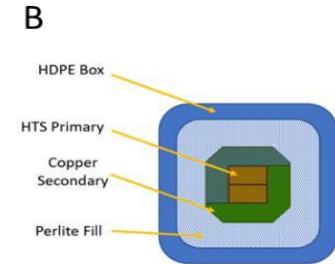


Figure 30. Thermal design of the main vessel.

[A] The MACE main coils (primary and secondary, as well as cryocooler cold head and heat sink materials are contained within a vessel. Vessel lid is shown as transparent, and the packed perlite fill is not

HDPE shown.



[B] Cross section diagram of the MACE and primary coil structures located within the main vessel. The coils are supported packed bet of evacuated perlite fill.

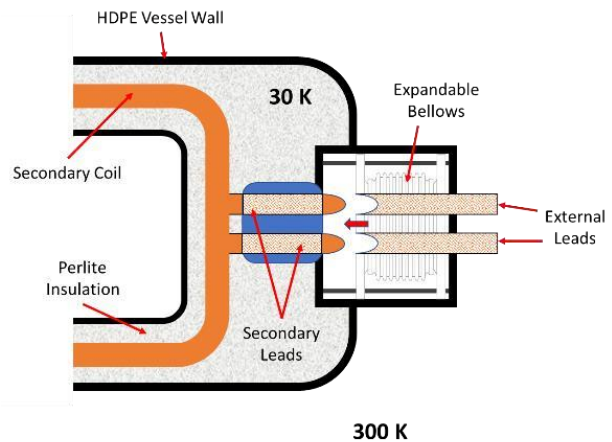
secondary with a

With the above design, under steady-state conditions, ISIT can expect a continuous heat load of 11 W into the secondary coil from the ambient exterior well within the cooling capacity of the cryocooler (see Section 5, Page14).

5.4.4 Thermal Design of Secondary Leads

The leads from the secondary coil in the 30 K compartment to the exterior (i.e. 300 K) of the vessel represent a significant thermal design challenge. The leads must be large enough to carry the expected current (up to 150,000 A) without excessive heating while simultaneously not being so large as to allow significant heat flux from the exterior of the vessel into the 30 K compartment and conductively heating the secondary and primary coils excessively. Additionally, to minimize heat flux into the 30 K compartment and to avoid conductively heating the secondary and primary

coils, it seems necessary that the external leads 10 cm-long Litz wire leads which connect to (connected to an external load such as a railgun) should remain physically unconnected (except at time of firing) to the leads within the 30 K compartment that are connected to the secondary coil. To accomplish these design objectives, ISIT has designed a demountable secondary lead system shown in the diagram in Figure 31. Although this design has not been brought into the CAD design as yet, ISIT believes it represents a viable method to satisfy all the design criteria for the secondary leads.



The secondary lead design specifies the use of

Figure 31. Thermal Design of Secondary Leads. To avoid excess heat flux from 300 K exterior into the 30 K interior compartment, the secondary leads can be quickly attached and detached from the external leads by means of an expandable bellows.

copper terminals on the secondary coil at one end and connect to bullet-type terminal pins at the other end that reside within the 30 K compartment (i.e. they are not physically connected to any outside leads). At 1 second before firing, a bellows holding the external leads is collapsed so that the bullet pins of the secondary leads are mated with a matching connector that terminates the external leads to the external wall of the main vessel. After firing, the bellows are expanded and the secondary leads are uncoupled from the connector containing the external leads. Thus, a physical connection from the 30 K region via the secondary leads to the 300 K region is only maintained for a few seconds during firing, and conductive heat losses are minimized.

The Litz wire leads (each of which has a cross-sectional area of 1-cm) are encased in an epoxy composite form to add rigidity to the structure.

5.4.5 Thermal cycling times for primary and secondary coil

The thermal cycling time for the main vessel of the MACE Experimental Demonstrator is

$$T = \frac{E}{P}$$

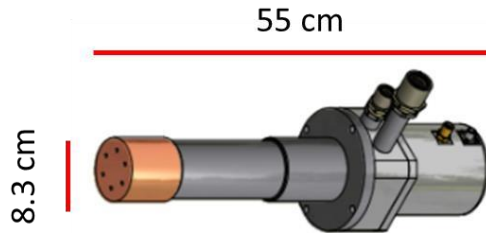
where, T is time in seconds, E is the thermal energy deposited into the structure during firing, and P is the available thermal cooling power provided by the cryocooler. During firing of the MACE Experimental Demonstrator, approximately 950 J of thermal energy is deposited into the secondary coil structure due to I²R losses of current passing through the 30 K coil and 330 J of thermal energy is deposited in the secondary leads attached to the secondary coil for a total of 1250 J of thermal energy which must be removed before the system returns to its pre-firing state. The available thermal power from the cryocooler is estimated to be 45 W(th), which equates to its 60 W(th) capacity (at 30 K) minus the steady-state losses of approximately 15 W(th) due to heat leakage into the 30 K compartment. Thus, expected cycling time will require at least 1250 J / 45 (J/s) = 27.8 s.

5.4.6 Thermal cycling times for persistent high temperature superconducting switch The HTS switch is expected to experience the highest transient thermal loads at time of firing since the switch must dissipate approximately 10% of the total stored energy in the MACE Experimental Demonstrator, or approximately 1.9 kJ of energy, it is expected the switch will experience a significant rise in temperature ($\Delta T = 75$ K). However, since the HTS switch coil (described in Tech Report 3) is mounted within a perforated copper coil form which allows the free circulation of sub-cooled liquid nitrogen (T = 70 K) to bathe the HTS switch coil, it is expected that the liquid nitrogen will remove the excess heat within seconds. Liquid nitrogen has a high heat of vaporization of 200,000 J / kg. Thus, removing 1920 J of heat from the HTS switch will consume only about 1 g of LN2. Also, LN2 can remove heat from a material at a rate of 10 W/cm² of material being cooled. Since the area of HTS tape in contact with LN2 is 80 cm², it is expected that the thermal cycling time of the HTS switch will be 1920 J / (80 * 10) (J/sec) = 2.4 s.

5.4.7 Cryocooler equipment, cryogen, and thermal insulation requirements

ISIT thermal management design will use standard, commercially available components and materials. For example, the cryocooler will most likely be a Cryomech AL230 (Figure 32), which provides approximately 60 W(th) cooling power at 30 K.

A



B

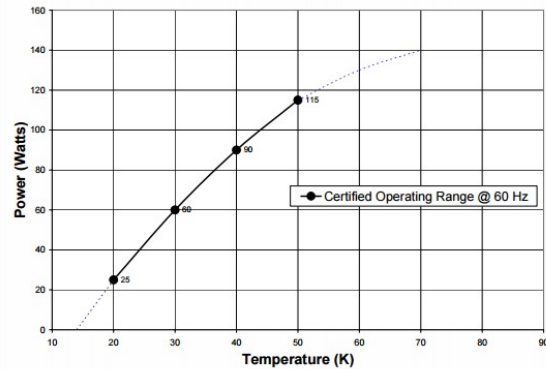


Figure 32. [A] The Cryomech AL230 cryocooler. [B] The cooling capacity of the AL230 at different temperatures.

Credit for both images: www.cryomech.com

5.5 STRUCTURAL ANALYSIS

5.5.1 Finite Element Analysis of Structure

Stress analysis of the primary/secondary coil assembly was performed using the structural FEA tool within Autodesk Inventor 2017 (Figure 33). The main concern here was that magnetic pressures generated during operation of the device would be strong enough to force significant deflections in the coil form structure, thereby generating strain on the HTS superconducting tape within the primary coil. The FEA simulation shows that a maximum deflection of 0.017 in occurs at the midpoint of the long edges of the coil. This generates a strain of only 0.00005%, or much less than the 0.1% strain tolerance of the HTS tape.

An analysis of deflection in the polymer vacuum vessel (Figure 34) showed negligible deflection throughout most of the structure. However, the large enclosed volume containing the cryocooler, leads, and other components showed enough deflection to justify adding two support pillars within the volume to maintain the integrity of the structure and ensure a good vacuum seal.

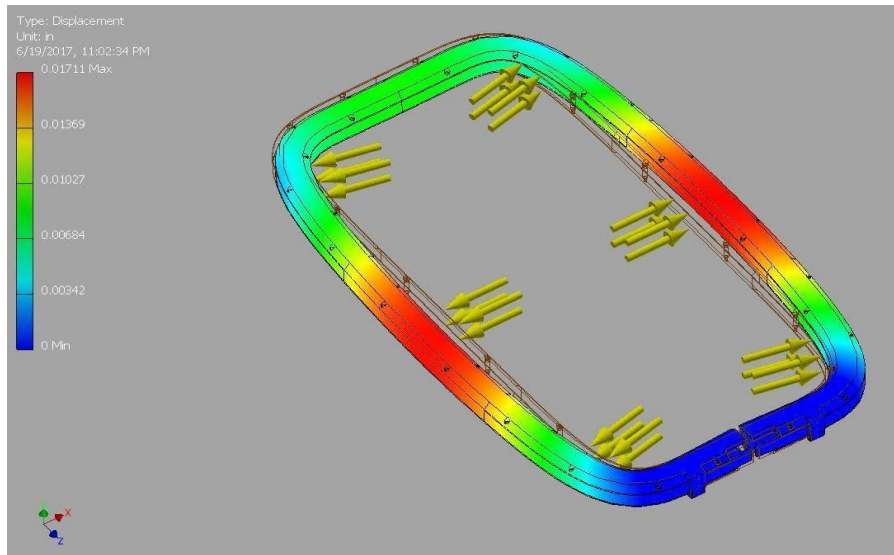


Figure 33. Deflection under load during operation of the primary/secondary coil assembly.

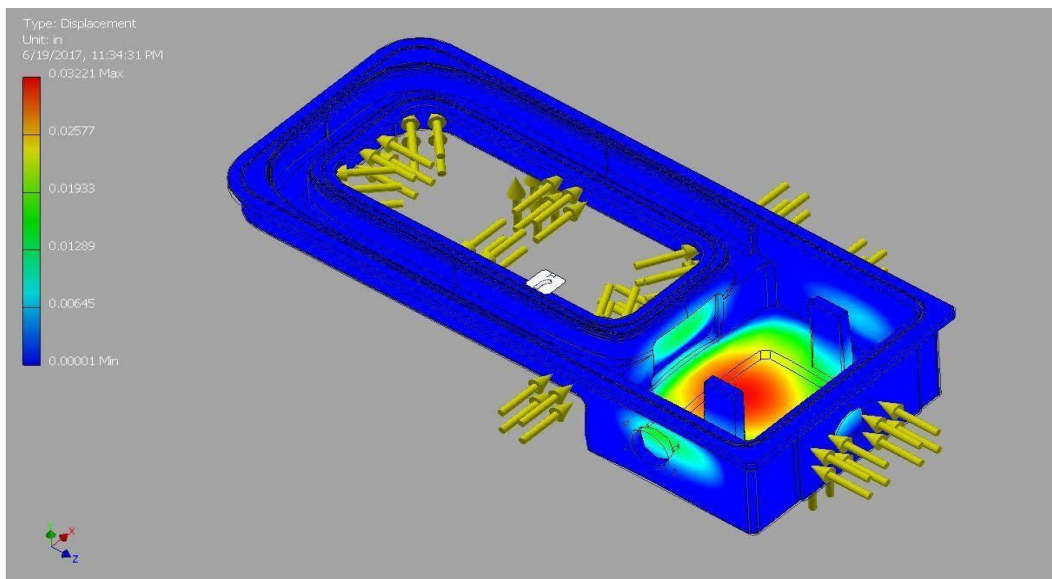


Figure 34. Deflection of vacuum vessel under atmospheric pressure.

6 SIGNIFICANT HARDWARE DEVELOPMENT

No physical hardware development occurred during this period since Phase I was only a feasibility study of the MACE concept. ISIT did create, however, a full CAD model of the MACE Demonstration Unit which will be built in a future Phase II of the MACE program.

7 SPECIAL COMMENTS

None.

8 IMPLICATIONS FOR FURTHER RESEARCH

The conclusions from the Phase I Feasibility Study of the MACE concept indicate that the annular SPPT design represents a significant improvement in the state of the art for SPPTs.

8.1 MACE PROTOTYPE DEVELOPMENT ROADMAP

In our initial proposal for the MACE program, ISIT proposed that after completing the Phase I Feasibility Study ISIT would then proceed to building prototypes in Phases II and III (see Figures 35 and 36). Phase II (“Option 1” in the proposal) is a 12-month program to build the MACE Demonstration Unit described in this report. Phase III (“Option 2” in the proposal) is an 18-month program to build the MACE Field Prototype which would be a realistic test of the MACE concept under field conditions. The MACE Field Prototype would deliver 10 MJ of energy with 90% efficiency in under 10 msec to a realistic external load (most likely a railgun). Additionally, the MACE Field Prototype will be in a toroidal configuration that would minimize external magnetic fringe fields so that the unit could be operated in close proximity to personnel and sensitive equipment.

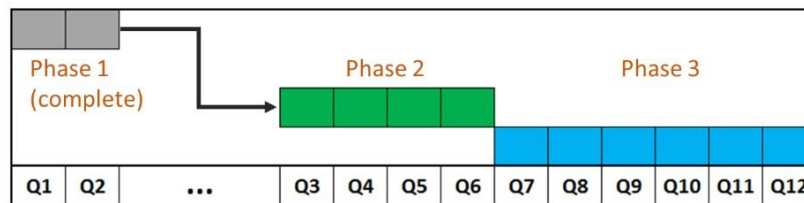


Figure 35. Duration of Phase 2 and Phase 3



	PHASE 2 MACE Demonstration Unit	PHASE 3 MACE Field Prototype
Operating Temperature	Primary: 30 K Secondary 30K	Primary: 30K Secondary: 70K (LN2 cooled)
Field Strength	2 Tesla	7 Tesla
geometry	simple loop	toroid (8 modular sections)
fringe fields?	Yes	no
energy transfer to load	80%	90%
amps	800	15,000
turns	188	116 X 8 = 930
switching	single HTS switch	hybrid HTS/tbd

Figure 36. MACE Design Targets for Phase 2 and Phase 3

Originally, Phase II was envisioned to begin immediately following the completion of Phase I. However, the project is currently talking with potential funding agencies that might be willing to contribute funds to Phases II and III.

8.2 PHASE 2: KEY SUPPLIERS, SUBCONTRACTORS, AND FACILITIES

During Phase I, ISIT identified key suppliers, subcontractors, and facilities that would be required to complete Phase II.

8.2.1 HTS Supplier [SuperPower Inc.](#)

450 Duane Avenue
Schenectady, NY 12304 USA

8.2.2 Coil Winding [HTS-110](#)

1B Quadrant Drive
Lower Hutt 5010
New Zealand

Or

SuperPower Inc.
450 Duane Avenue
Schenectady, NY 12304 USA

8.2.3 Coil Form and Dewar Manufacture [Atlas Technologies](#)

305 Glen Cove Road
Port Townsend, WA 98368 USA

8.2.4 Cryocooler [Cryomech, Inc.](#)

113 Falso Drive
Syracuse, NY 13211 USA

8.2.5 Main Unit Vacuum Vessel Marine
Science Development Center
Scripps Institution of Oceanography
9500 Gilman Drive
La Jolla, CA 92093 USA